Above-threshold multiphoton detachment from the H^- ion by 10.6-μm radiation: Angular distributions and partial widths

Dmitry A. Telnov* and Shih-I Chu
Department of Chemistry, University of Kansas, Lawrence, Kansas 66045
(Received 3 June 1994)

We present a general procedure for accurate nonperturbative treatment of the angular distribution and partial widths for multiphoton above-threshold detachment (ATD) of atoms or negative ions in intense laser fields. The procedure consists of the following two steps: (1) The resonance wave function is determined by means of the non-Hermitian Floquet Hamiltonian method. The Floquet Hamiltonian is discretized by the complex scaling generalized pseudospectral method recently developed by Yao and Chu [Chem. Phys. Lett. **204**, 381 (1993)]. No computation of potential matrix elements is required, and the kinetic-energy matrix elements can be evaluated analytically. (2) The angular distribution and partial rates are calculated, based on an exact differential expression, and a procedure is developed for the backrotation of the total complex resonance wave function to the real axis. The method is applied to the study of multiphoton ATD of H^- in strong fields at 10.6 μm. An accurate one-electron model potential [Laughlin and Chu, Phys. Rev. A **48**, 4654 (1993)], which reproduces the known H^- binding energy and the low-energy e-H($1s$) elastic scattering phase shifts, is employed. At this low frequency, the resonance wave functions can be obtained efficiently and rather accurately by means of a nonperturbative adiabatic approach recently developed by Telnov [J. Phys. B **24**, 2967 (1991)]. This adiabatic theory is also valid in the limit of weak fields, and its validation is justified by its agreement with the exact perturbation calculations for the seven- and eight-photon detachment of H^-. Detailed results for the angular distribution and partial widths for multiphoton ATD of H^- are presented for the moderately strong laser intensity regime (10^{10}–10^{11} W/cm^2) at 10.6 μm.

PACS number(s): 32.80.Rm, 32.80.Fb, 42.50.Hz

I. INTRODUCTION

Recently there has been considerable interest both experimentally [1–3] and theoretically [4–6] in the study of multiphoton detachment of H^-. The H^- ion is one of the simplest yet delicate three-body systems and possesses only one bound state. For moderate laser intensities used in recent experiments (10^9–10^{11} W/cm^2), structure far above the ionization threshold can be safely ignored. This simplifying feature renders the multiphoton detachment of H^- a unique and fundamental process to study. In this paper we present the first theoretical study on the angular distribution and partial widths for multiphoton above-threshold detachment (ATD) of H^-.

The H^- ion is described by an accurate one-electron model recently constructed [5] to reproduce both the exact experimental binding energy [7] and the low-energy e-H($1s$) elastic phase shifts [8]. The one-photon photodetachment cross sections based on this model potential are in excellent agreement with earlier accurate correlated two-electron calculations [9]. The H^- model potential has been employed to study the generalized two- to eight-photon detachment cross sections based on the lowest-nonvanishing-order perturbation theory and the solution of the associated set of inhomogeneous differential equations [5]. More recently the H^- model potential has been used to study the intensity-dependent multiphoton detachment rates in nonperturbative regimes [6]. A complex-scaling generalized pseudospectral (CSGP) technique [6,10] is introduced to discretize and facilitate the solution of the time-independent non-Hermitian Floquet Hamiltonian [11,12] for the complex quasienergies. A simulation of the intensity-averaged multiphoton detachment rates is achieved by considering the experimental conditions of the laser and H^- beams. The results [6] (without any free parameters) are in good agreement with the experimental data [3], both in the absolute magnitude and in the threshold behavior.

The motivations and outline of this paper are described as follows. (i) First, we extend our recent nonperturbative study of the total multiphoton detachment rates of H^- [6] to the detailed study of angular distribution and partial widths associated with the ATD processes. Experimental study of ATD processes is being planned [13]. Such a theoretical study can provide insights regarding the feasibility of observing the ATD phenomena. (ii) The determination of angular distribution and partial widths are by no means straightforward. In this paper, we present a new procedure for accurate calculation of both angular distribution and partial widths based on a back rotation of the total resonance wave functions to the real axis and an exact differential formula [14]. The (complex-quasienergy) resonance wave functions are obtained by the solution of the non-Hermitian Floquet

*Permanent address: Institute of Physics, St. Petersburg State University, 198904 St. Petersburg, Russia.

Hamiltonian and the use of the CSGP technique. The CSGP procedure does not require the computation of potential matrix elements and is computationally simpler and faster than the conventional basis-set expansion-variational methods. The advantages and usefulness of this method have been discussed in [6,10]. (iii) For laser frequency smaller than the photodetachment binding energy, such as the CO_2 laser wavelength 10.6 μm used in the experiments of Tang and co-workers [1–3], approximate yet accurate resonance wave functions can be also obtained by the nonperturbative adiabatic theory recently developed [14]. We examine the validity of the adiabatic theory in both weak and nonperturbative regimes by comparing the adiabatic results with exact perturbation [5] and Floquet calculations [6], respectively. We then apply the adiabatic theory to obtain the detailed angular distribution and partial widths for multiphoton ATD of H^- at three moderate strong laser intensities: 10^{10}, 5×10^{10}, and 10^{11} W/cm^2.

We begin in Sec. II the presentation of the general theory for electron distributions, the adiabatic wave functions, and a new procedure for obtaining the angular distributions and partial widths. Section III presents the main numerical results for ATD of H^- at 10.6 μm. This is followed by a conclusion in Sec. IV.

II. THEORY

A. General expressions for the electron distributions

We make use of the Floquet solution $\Psi(\mathbf{r},t)$ of the time-dependent Schrödinger equation (atomic units will be used throughout the paper):

$$i\frac{\partial}{\partial t}\Psi(\mathbf{r},t)=[-\tfrac{1}{2}\nabla^2+W(r)+\mathbf{F}\cdot\mathbf{r}\cos\omega t]\Psi(\mathbf{r},t)\ , \tag{1}$$

where $\Psi(\mathbf{r},t)$ is the quasienergy wave function in the length gauge; $W(r)$ is the accurate one-electron H^- model potential (see [5,6]); $\mathbf{F}$ and ω are, respectively, the laser field strength and frequency [linear polarization of the laser field is assumed in Eq. (1)]. The wave function $\Psi(\mathbf{r},t)$ can be represented as

$$\begin{aligned}&\Psi(\mathbf{r},t)=\exp(-i\varepsilon t)\psi(\mathbf{r},t)\ ,\\ &\psi(\mathbf{r},t)=\psi(\mathbf{r},t+2\pi/\omega)\ ,\end{aligned} \tag{2}$$

ε being the quasienergy. If the wave function $\Psi(\mathbf{r},t)$ describes the decay process (outgoing wave boundary conditions) then the quasienergy is complex with the absolute value of the imaginary part equal to the half of the total width. It is well known that the quasienergy is defined modulo ω; we choose it as a continuous function of the field amplitude F with the zero-field limit equal to the unperturbed energy value E^0:

$$\varepsilon\to E^0\quad(F\to0)\ . \tag{3}$$

The periodically time-dependent wave function $\psi(\mathbf{r},t)$ can be expanded in a Fourier series:

$$\psi(\mathbf{r},t)=\sum_m\psi_m(\mathbf{r})\exp(-im\omega t)\ . \tag{4}$$

In the $F\to0$ limit the Fourier component $m=0$ corresponds to the unperturbed wave function.

Our method of evaluating the electron distributions is based on the following *exact* expression for the differential electron flux [14]

$$\frac{1}{\sin\vartheta}\frac{d\Gamma_n}{d\vartheta}=\frac{1}{2\pi}k_n|A_n|^2\ , \tag{5}$$

where the n-photon detachment amplitude A_n is defined as follows:

$$\begin{aligned}A_n=&\frac{1}{2\pi}\int_{-\pi}^{\pi}d\tau\exp[in\tau-i\tfrac{1}{8}F^2\omega^{-3}\sin2\tau+iF\omega^{-2}k_n\cos\vartheta\cos\tau]\\ &\times\int d^3r'\exp\left[i\frac{(\mathbf{F}\cdot\mathbf{r}')}{\omega}\sin\tau-ik_n(\hat{\mathbf{r}}\cdot\mathbf{r}')\right]W(r')\psi(\mathbf{r}',\tau/\omega)\ .\end{aligned} \tag{6}$$

This expression is extracted from the exact integral equation for the decay wave function $\psi(\mathbf{r},t)$, the latter equation being obtained with the help of the Green function for the motion in the uniform ac field (see [14]).

The physical meaning of the left-hand side in Eq. (5) is the flux density (Γ_n is the partial width) of the electrons detached from the ion with the absorption of n photons and ejected under the angle ϑ with respect to the field vector $\mathbf{F}$ direction. On the right-hand side, k_n is the electron drift momentum defined as

$$k_n=\sqrt{2(\mathrm{Re}E_n-U_p)}\ , \tag{7}$$

where

$$E_n=\varepsilon+n\omega \tag{8}$$

is the electron energy after absorption of n photons, and

$$U_p=F^2(2\omega)^{-2} \tag{9}$$

is the mean oscillation energy (equal to the ponderomotive potential). The detachment is possible only if $\mathrm{Re}E_n>U_p$; from this inequality one can extract $n_{\min}$—the minimal number of photons required for detachment. With the increase of the laser field strength F, the minimal number of photons $n_{\min}$ also increases due to the increase of the positive ponderomotive energy shift of the detachment threshold.

In Eq. (6), $\hat{\mathbf{r}}$ is the unit vector in the direction of the electron ejection. In the spherical coordinate system with the z polar axis along the vector $\mathbf{F}$, $\hat{\mathbf{r}}$ is defined by the polar angle ϑ and azimuthal angle φ. However, for the spherically symmetrical potential W and the initial state with definite angular momentum and its z projection, the

electron distributions do not depend on the angle φ. This fact is already taken into account in Eq. (5) where the integration over φ is performed. So, the partial widths Γ_n representing the energy spectrum are obtained from (5) by integration over the angle ϑ:

$$\Gamma_n = \int_0^\pi d\vartheta \frac{d\Gamma_n}{d\vartheta} = \frac{1}{2\pi} k_n \int_0^\pi d\vartheta \sin\vartheta |A_n|^2 . \quad (10)$$

The total width Γ is the sum of Γ_n for those n corresponding to the open channels:

$$\Gamma = \sum_{n=n_{\min}}^{\infty} \Gamma_n . \quad (11)$$

Certainly, the correct results for the electron distributions are given by Eqs. (5) and (10) if the wave function $\psi(\mathbf{r},t)$ is normalized to unit probability. The normalization of the wave function $\psi(\mathbf{r},t)$ is not straightforward because it represents a resonance state with the complex quasienergy and diverges exponentially as $r \to \infty$. However, if the decay rate is small enough (and any Floquet theory is applicable, at least, if the decay during one field cycle is negligible), a number of simple and consistent normalization procedures can be suggested. The discussion of the normalization problem as well as the deduction of Eq. (5) based on the Green-function method can be found in Ref. [14]. In the present paper we adopt the normalization procedure based on the normalization integral without complex conjugated radial wave functions. Such an integral may be analytically continued in the complex r-coordinate plane (where the wave function vanishes at infinity) and evaluated by the usual methods. The error inserted by such a procedure is of the order of squared total width and is negligible for the laser intensities under consideration.

Using the Fourier expansion (4), one can represent the amplitude A_n in the following form:

$$A_n = \sum_m \int d^3r' \exp[-ik_n(\hat{\mathbf{r}}\cdot\mathbf{r}')] A_n^{(m)}(\mathbf{r}') W(r') \times \psi_m(\mathbf{r}') , \quad (12)$$

where

$$A_n^{(m)}(\mathbf{r}') = \frac{1}{2\pi} \int_{-\pi}^{\pi} d\tau \exp[i\chi_{mn}(\tau,\mathbf{r}')] , \quad (13)$$

and

$$\chi_{mn}(\tau,\mathbf{r}') = (n-m)\tau - \tfrac{1}{8}F^2\omega^{-3}\sin 2\tau + F\omega^{-2}k_n \cos\vartheta \cos\tau + \frac{(\mathbf{F}\cdot\mathbf{r}')}{\omega}\sin\tau . \quad (14)$$

Integration over the τ variable in (13) can be performed exactly, the result being expressed via the Bessel functions:

$$A_n^{(m)}(\mathbf{r}') = \sum_{p=-\infty}^{\infty} i^{p-m} \mathcal{J}_{n-m-p}(F^2(2\omega)^{-3}, F\omega^{-2}k_n \cos\vartheta) \times J_p\left[\frac{(\mathbf{F}\cdot\mathbf{r}')}{\omega}\right] , \quad (15)$$

where $J_n(x)$ is the ordinary Bessel function, and the generalized Bessel function $\mathcal{J}_n(x,y)$ is defined as follows:

$$\mathcal{J}_n(x,y) = \sum_{s=-\infty}^{\infty} (-1)^s J_s(x) J_{n-2s}(y) . \quad (16)$$

B. Adiabatic ansatz for the wave function

The expressions for the electron angular and energy distributions written above are *exact* within the framework of the Floquet theory. However, since the analytical exact solution of Eq. (1) does not exist and numerical solution requires large-scale computations [6] we look into some approximate (yet accurate) solution for the wave function. For multiphoton ionization or detachment processes the adiabatic theory [14,15] can be used. This theory implies that the radiation frequency is small compared with the ionization potential but enables *nonperturbative* treatment of the external field. Adiabatic theory suggests the following ansatz for the wave function (Fourier component) $\psi_m(\mathbf{r})$ in Eq. (4):

$$\psi_m(\mathbf{r}) = C_m[\Phi(E_m,\gamma_m,\mathbf{r}) + (-1)^m \Phi(E_m,\gamma_m,-\mathbf{r})] , \quad (17)$$

where $\gamma_m = \gamma(E_m)$, $E_m = \varepsilon + m\omega$, and the functions $\gamma(E)$ and $\Phi(E,\gamma(E),\mathbf{r})$ are found by solving the time-independent equation

$$[-\tfrac{1}{2}\nabla^2 + W(r) + \gamma(E)(\mathbf{F}\cdot\mathbf{r})]\Phi(E,\gamma(E),\mathbf{r}) = E\Phi(E,\gamma(E),\mathbf{r}) . \quad (18)$$

In Eq. (18) the energy value E is fixed and the $\gamma(E)$ value is obtained as an eigenvalue depending on E as a parameter (outgoing wave boundary conditions are assumed). For real E, $\gamma(E)$ is complex, and *vice versa*, reflecting the possibility of tunneling decay in the static field. The ansatz (17) preserves the proper spatial parity of the Fourier components $\psi_m(\mathbf{r})$ following from the exact symmetry of the time-dependent Schrödinger equation (1) with respect to the discrete transformation $\mathbf{r} \to -\mathbf{r}$, $t \to t + 2\pi/\omega$. The details concerning the deduction of Eq. (17) can be found in Ref. [15]. The coefficients C_m in Eq. (17) satisfy the three-term recursion relations:

$$C_{2m-2} + C_{2m+2} = 2(2\gamma_{2m}^2 - 1)C_{2m} , \quad (19)$$

$$C_{2m+1} = \frac{1}{2\gamma_{2m+1}}(C_{2m} + C_{2m+2}) . \quad (20)$$

One should impose zero boundary conditions on C_{2m} as $m \to \pm\infty$. Then Eq. (19) is an eigenvalue problem for the quasienergy ε since γ_{2m} depends on $E_{2m} = \varepsilon + 2m\omega$. After solving the Eq. (19), the value $\mathrm{Re}\varepsilon$ describes the ac Stark shifted energy level (in low-frequency limit) and $\mathrm{Im}\varepsilon$ provides the tunneling decay rate. The latter should be discarded because the correct total detachment rate in the ac field is given by Eq. (11) and can be obtained after the calculation of the electron energy distribution. The equations (19) and (20) imply the normalization of the

function $\Phi(E,\gamma,\mathbf{r})$ in the following way:

$$\int d^3r\,\Phi^2(E,\gamma(E),\mathbf{r})=\gamma(E)\frac{d\gamma(E)}{dE}\ . \tag{21}$$

An arbitrary multiplier that appears in the solutions of Eqs. (19) and (20) should be chosen to ensure the normalization of the total wave function (4) to unity [14].

C. Generalized complex-scaling pseudospectral method and reverse complex scaling of the resonance wave function: procedure for the determination of the partial widths

The solution of the complex eigenvectors in Eq. (18) can be greatly facilitated by the use of the complex rotation [6] of the r coordinate, $r\rightarrow r\exp(i\alpha)$, since for real r the function $\Phi(E,\gamma(E),\mathbf{r})$ manifests exponential divergence as $r\rightarrow\infty$ and cannot be subject to unique boundary conditions. We use the complex-scaling generalized pseudospectral method recently developed [6,10]. Briefly, after Eq. (18) is complex rotated, we discretize the radial coordinate r by the generalized pseudospectral technique, and a nonlinear algebraic mapping [see Eq. (26) below] is applied to substitute a finite coordinate interval for the infinite r semiaxis. Such a mapping gives a larger density of collocation points near $r=0$, which enables more accurate description of the Coulomb and centrifugal potential singular behavior near the origin. The background and details of the method can be found elsewhere [6]. Here we recollect the principal equations only and describe an alternative procedure for obtaining the partial widths from the complex-rotated wave functions. All the equations below assume that the coordinate r has already been complex rotated.

Equation (18) is really two dimensional since the projection of the angular momentum onto the field axis is an integral of motion. Introducing the spherical coordinate system (r,ϑ,φ) with the polar axis along the field $\mathbf{F}$ direction one can write

$$\Phi(E_m,\gamma_m,\mathbf{r})=\exp(iM\varphi)r^{-1}\phi_m(r,\cos\vartheta)\ . \tag{22}$$

Here M is the projection of the angular momentum on the field axis; below we consider $M=0$ as it is for the detachment from the H^- ion. The function $\phi_m(r,\cos\vartheta)$ depends on r and ϑ only and (as a function of ϑ) can be expanded in the series of Legendre polynomials:

$$\phi_m(r,\cos\vartheta)=\sum_{l=0}^{\infty}\sqrt{2l+1}\,\phi_{ml}(r)P_l(\cos\vartheta)\ . \tag{23}$$

As our calculations show, for laser intensities 10^{10}–10^{11} W/cm^2 (of current experimental interests [3]) one has to retain no more than ten angular momenta in the sum (23) to achieve convergence. The functions $\phi_{ml}(r)$ with different l constitute an eigenvector of the complex symmetric Hamiltonian defined as follows:

$$\mathcal{H}_{l,l}=-\frac{1}{2}\frac{d^2}{dr^2}+W(r)+\frac{l(l+1)}{2r^2}\ ,$$
$$\mathcal{H}_{l+1,l}=\mathcal{H}_{l,l+1}=(l+1)[(2l+1)(2l+3)]^{-1/2}\gamma_m Fr\ . \tag{24}$$

According to the complex-scaling generalized pseudospectral method [6], the Hamiltonian (24) is discretized on a set of collocation grid space points, the potential matrix elements being diagonal. The kinetic-energy operator matrix elements can be evaluated analytically. As discussed elsewhere [6], this procedure is computationally more efficient than the traditional basis-set expansion method. The approximation $\tilde{\phi}_{ml}(r)$ for the function $\phi_{ml}(r)$ is represented by the following sum via its values on a set of collocation points r_j:

$$\tilde{\phi}_{ml}(r)=\sum_{j=0}^{N}\frac{[P_{N+1}(x)-P_{N-1}(x)](1-x_j)}{(2N+1)(x-x_j)(1-x)P_N(x_j)}\phi_{ml}(r_j)\ . \tag{25}$$

Here $P_N(x)$ is the Legendre polynomial; the collocation points x_j (and corresponding points r_j in the r variable) are the zeros of the derivative $P'_N(x)$, and $j=0$ and $j=N$ correspond to $x=-1$ and $x=1$, respectively. The variable x scans the interval $[-1,1]$ and is related to $r\in[0,\infty]$ as follows:

$$r=R\left[\frac{1+x}{1-x}\right]\exp(i\alpha)\ , \tag{26}$$

where R is a real scaling parameter and α is the angle of complex rotation. The complex-scaling generalized pseudospectral method reduces the differential equation with the Hamiltonian (24) to a non-Hermitian matrix eigenvalue problem for the vector $\{\phi_{ml}(r_j)\}$. Since the wave function under consideration describes a resonance state and increases exponentially for real $r\rightarrow\infty$, the angle of complex rotation α should be positive to ensure stability of the method, so the function is obtained on the ray in the complex r plane where it vanishes as $r\rightarrow\infty$.

The functions $\tilde{\phi}_{ml}(r)$ and $\phi_{ml}(r)$ have the same values at $r=r_j$, so Eq. (25) may be considered as an interpolation formula. The greater the order N of the Legendre polynomial, the better the approximation (25). However, this interpolation originally gives the values of the eigenfunction on the ray defined by the angle α in the complex r plane, whereas to calculate the distributions one needs the wave function for real r. [See Eqs. (12)–(15): for complex r the functions to be integrated increase exponentially with $r\rightarrow\infty$.] To avoid this difficulty one should rotate the wave function back to the real r axis. An important point which is not clear *a priori* is that such a back rotation may be performed with the approximate expression (25). To get the wave function for *real* r one has to insert in (25) *complex* x values defined by the equation,

$$x=\frac{r\exp(-i\alpha)-R}{r\exp(-i\alpha)+R}\ . \tag{27}$$

As our test calculations show, the resulting wave function is an excellent approximation to the eigenfunction on the real r range, which is important for the calculation of the electron angular distributions and partial widths. Finally, we note that the reverse complex-scaling technique described here can be also applied directly to the exact wave function in Eq. (6), providing an alternative pro-

cedure for accurate determination of partial widths from the total exact (complex-rotated) wave function.

III. RESULTS

A. Weak-field limit

Unlike the Keldysh-Faisal-Reiss theories [16] and their modified versions, which are used to describe tunnel multiphoton detachment of the electron bound in the short-range potential but give incorrect results in the perturbation regime, the adiabatic theory has no formal limitations from the weak external fields. To test the accuracy of the adiabatic theory in this limit, we performed the calculations of detachment rates for weak external fields to obtain generalized cross sections. The cross sections were calculated for a number of frequency values corresponding to eight-photon detachment for which the exact perturbation-theory results were obtained earlier [5] (by means of an extension of the Dalgarno-Lewis inhomogeneous differential equation approach [17]) with the same model potential. The results are presented in Fig. 1. They show general good agreement (within a few percent) between the perturbation and adiabatic theories, justifying the validity of the adiabatic approach. In the following we also present the numerical data for the generalized seven-photon detachment cross section $\sigma^{(7)}$ obtained for the 10.6-μm radiation of the CO_2 laser used in the Los Alamos experiments [3]. As one can see, the perturbation theory [18] and adiabatic theory differ by no more than 2%:

$$\sigma^{(7)}=3.571\times10^{-200}\ \text{cm}^{14}\text{s}^{6}\ \text{(perturbation theory)},$$
$$\sigma^{(7)}=3.639\times10^{-200}\ \text{cm}^{14}\text{s}^{6}\ \text{(adiabatic theory)}. \quad (28)$$

B. Comparison with accurate Floquet calculations

To test our procedure for the determination of partial rates from the complex-rotated wave functions, we performed the calculations of partial widths with accurate Floquet wave functions (without adiabatic ansatz) for the case of three-photon dominant electron detachment. The accurate total widths in this case are available in Ref. [6]. The results are shown in Table I for two sets of the external field parameters (frequency and intensity). One can see an excellent agreement (within 0.6%) between the total rates obtained by accurate Floquet calculations (diagonalization of the non-Hermitian Floquet matrix) and by the procedure based on Eq. (11) and described in Sec. II C. These results justify our present procedure for the determination of partial widths using the reverse complex scaling of the wave functions. We should stress the stability of this procedure. According to Eq. (6) the wave function is required in the core region where the computed data are the most reliable. Unlike the method of Ref. [19] we do not need to investigate the asymptote of the complex rotated wave function where it decreases exponentially and may be perturbed strongly by the computational errors.

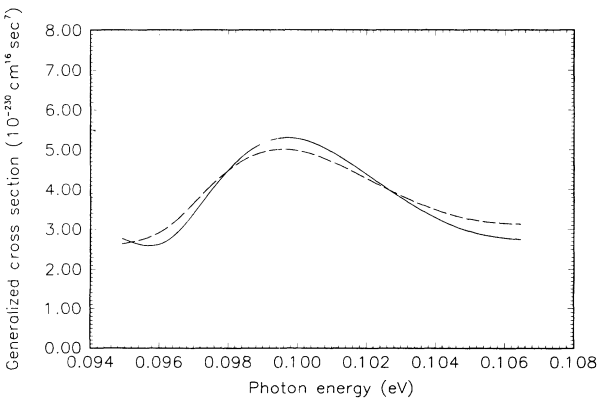

FIG. 1. Generalized cross sections for eight-photon detachment (in units of 10^{-230} cm^{16}s^{7}). Solid curve: adiabatic theory, present paper; dashed curve: perturbation theory [5].

C. Energy and angular distributions for above-threshold multiphoton detachment of the electrons by intense 10.6-μm radiation

We present here the results of the calculation of multiphoton above-threshold detachment (ATD) by 10.6-μm radiation for the intensities $I=10^{10}$, 5×10^{10}, and 10^{11} W/cm^2. The 10.6 μm is the CO_2-laser laboratory wavelength used in a recent experiment by Tang *et al.* [3]. Even at the lowest intensity $I=10^{10}$ W/cm^2 considered here the detachment regime is already nonperturbative since the minimum number of photons required for the detachment is equal to 8, whereas the process is seven photon for the weak fields. Due to the shift of the detachment threshold in intense fields, the seven-photon channel is already closed and one peak in the electron energy spectrum switched off. For the intensities 5×10^{10} and 10^{11} W/cm^2, we find $n_{\min}=11$ and $n_{\min}=16$, respectively.

The energy spectra of the detached electrons are presented in Figs. 2–4 for the intensities 10^{10}, 5×10^{10}, and 10^{11} W/cm^2, respectively. For the lowest intensity $I=10^{10}$ W/cm^2 considered here (Fig. 2), the energy spectrum shows quite rapid decrease of the partial rates as the number of photons absorbed increases. The first peak in the spectrum ($n=n_{\min}=8$) is the highest, and only five to six peaks contribute significantly to the total rate. The medium strong $I=5\times10^{10}$ W/cm^2 case (Fig. 3) is a clear demonstration of the peak switching phenomenon. The first peak in the spectrum ($n=n_{\min}=11$) is very close to the threshold, and its intensity is already less than that of the second one. The nonperturbative behavior of the spectrum is also pronounced in the plateau near $n=14$–16 where the peaks have comparable heights. The strong-field detachment features are the most distinct for $I=10^{11}$ W/cm^2 (Fig. 4). The energy spectrum demonstrates a broad plateau where the partial rates decrease slowly with the increasing n (number of photons absorbed) showing nonmonotonous dependence on n. According to the adiabatic theory [14] the part of the energy spectrum with the smooth dependence on the number of absorbed photons has the scale $2U_p$.

The numerical data for the partial rates is presented in

TABLE I. Partial and total rates for three-photon dominant detachment. The rates labeled A are obtained from accurate Floquet wave functions by the procedure of Sec. II C. The total rates labeled B are obtained from direct diagonalization of the non-Hermitian Floquet Hamiltonian [6].

Frequency, (eV)	Intensity, (10^{10} W/cm^2)	Number of photons absorbed	Partial rates, (10^{-8} a.u.) A	Total rates (10^{-8} a.u.) A	B
0.276	0.8	3	7.271		
		4	0.258		
		5	0.007		
				7.536	7.564
0.357	3.6	3	128.4		
		4	9.762		
		5	0.861		
		6	0.058		
				139.1	139.9

Table II. The partial rates shown for the intensities 10^{10} and 5×10^{10} W/cm^2 constitute the converged result for the total rates, whereas for $I=10^{11}$ W/cm^2 a larger number of partial rates is required than can be placed in the table. So, the total rate for $I=10^{11}$ W/cm^2 is calculated from a larger number of partial rates than it is shown in Table II.

The angular distributions are presented in Figs. 5–7 for the angular range [0,90°] since they are symmetrical with respect to the transformation $\vartheta\to\pi-\vartheta$. The distributions show strong anisotropy, especially for high-energy ATD peaks. The electrons with the high energies are ejected in the directions close to that of the laser electric-field polarization vector. The decrease of partial rates with increasing n is achieved mainly due to narrowing the angular distribution, whereas the differential rates for the angles close to $\vartheta=0(\pi)$ demonstrate nonmonotonous dependence on n and are comparable in magnitude for a large number of ATD peaks (for example, $n=20$–26 for $I=10^{11}$ W/cm^2).

The anisotropy of angular distributions can help to observe ATD electrons in experiments. Thus, for $I=10^{10}$ W/cm^2 in the angular range $\pm20°$ around $\vartheta=0$ it is much more probable to detect the ATD electron with $n=9$ than the electron absorbed the minimal number of photons $n_{\min}=8$, whereas the partial rate for the latter is about 3.5 times greater.

For the tunneling detachment regime [$(\omega\sqrt{-2E^0}/F)\ll1$, E^0 being the electron energy in the initial state], which is to a great extent realized for $I=10^{11}$ W/cm^2, an approximate formula for the differential rate [Eqs. (5) and (6)] can be obtained

$$\frac{1}{\sin\vartheta}\frac{d\Gamma_n}{d\vartheta}\cong\frac{8\omega^2}{\pi}k_n(2\lambda_nF)^{-4/3}\left|\sum_m\cos\left[3U_p\omega^{-1}\mu_n\lambda_n-(n-m)\arctan(\lambda_n/\mu_n)-m\frac{\pi}{2}\right]\right.$$
$$\times\int d^3r'\exp\left[i\frac{(\mathbf{F}\cdot\mathbf{r}')}{\omega}\sin\tau-ik_n(\hat{\mathbf{r}}\cdot\mathbf{r}')\right]W(r')\psi_m(\mathbf{r}')$$
$$\left.\times\mathrm{Ai}\left[\frac{\kappa_{mn}^2+2\lambda_n(\mathbf{F}\cdot\mathbf{r}')}{(2\lambda_nF)^{2/3}}\right]\right|^2, \tag{29}$$

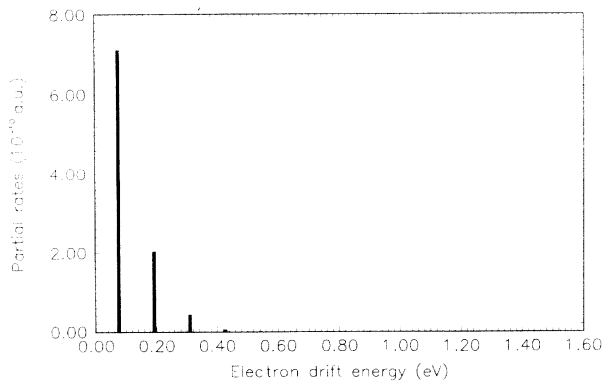

FIG. 2. Electron energy distribution after multiphoton above-threshold detachment by 10.6-μm, 10^{10} W/cm^2 radiation. The heights of the bars correspond to the partial rates after absorption of n photons, starting with $n_{\min}=8$.

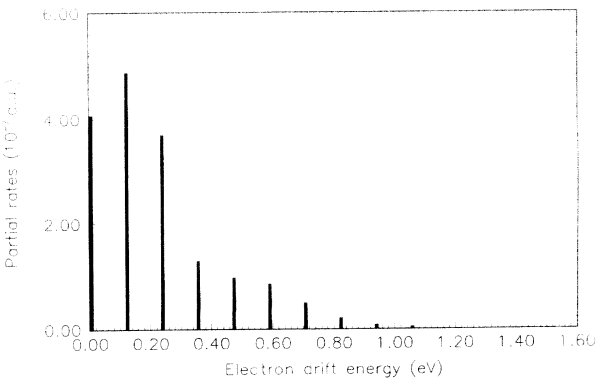

FIG. 3. The same as Fig. 2 for the intensity 5×10^{10} W/cm^2; $n_{\min}=11$.

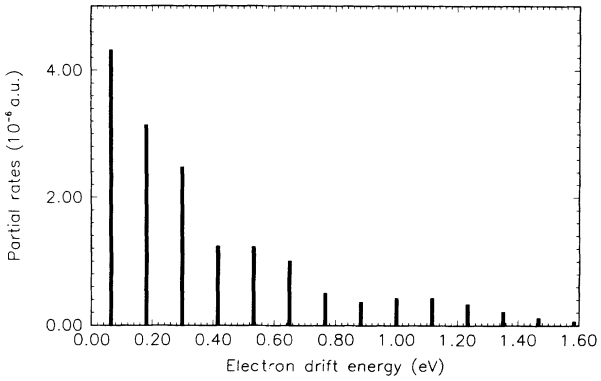

FIG. 4. The same as Fig. 2 for the intensity 10^{11} W/cm^2; $n_{\min}=16$.

where Ai(x) is the Airy function, and the following notations are used:

$$\mu_n=\omega F^{-1}k_n\cos\vartheta\ , \tag{30}$$

$$\lambda_n=\sqrt{1-\mu_n^2}\ , \tag{31}$$

$$\kappa_{mn}^2=k_n^2\sin^2\vartheta-2E_m\ . \tag{32}$$

The detailed theory of tunneling detachment and ionization containing the derivation of Eq. (29) will be presented elsewhere. Here we point out only that this equation is valid for $k_n^2<4U_p$, i.e., within the naturally scaled range for low-frequency detachment [14]. For moderate strong laser fields, the Fourier component $\psi_0(\mathbf{r})$ has the greatest weight in the sum over m in (29). Then, the oscillations in the angular distributions are governed mainly by the simple expression

$$\cos^2[3U_p\omega^{-1}\mu_n\lambda_n-n\arctan(\lambda_n/\mu_n)]\ , \tag{33}$$

the other terms in Eq. (29) being responsible for the absolute value. The comparison of the oscillatory behavior of (33) with the exact angular distributions following from Eqs. (5) and (6) and presented in Fig. 7 shows an excellent agreement with respect to the minima and maxima positions [note that the expression (33) preserves the zeros of the angular distributions at $\vartheta=90°$ for odd n, which follows from the exact equation (6)].

IV. CONCLUSION

In this paper, we have presented a general procedure for nonperturbative study of the angular distribution and partial widths for multiphoton above-threshold ionization of atoms or detachment of negative ions in intense laser fields. The method is based on the back rotation of

TABLE II. Partial rates for the detachment by 10.6-μm radiation.

Number of photons absorbed	Partial rates (a.u.)		
	$I=10^{10}$ W/cm^2	$I=5\times10^{10}$ W/cm^2	$I=10^{11}$ W/cm^2
8	0.7117×10^{-9}		
9	0.2034×10^{-9}		
10	0.4323×10^{-10}		
11	0.5258×10^{-11}	0.4074×10^{-6}	
12	0.7855×10^{-12}	0.4882×10^{-6}	
13	0.2270×10^{-12}	0.3692×10^{-6}	
14		0.1295×10^{-6}	
15		0.9716×10^{-7}	
16		0.8524×10^{-7}	0.4321×10^{-5}
17		0.4881×10^{-7}	0.3137×10^{-5}
18		0.2057×10^{-7}	0.2480×10^{-5}
19		0.7867×10^{-8}	0.1237×10^{-5}
20		0.3944×10^{-8}	0.1224×10^{-5}
21		0.2923×10^{-8}	0.1008×10^{-5}
22		0.2369×10^{-8}	0.5046×10^{-6}
23		0.1765×10^{-8}	0.3640×10^{-6}
24		0.1180×10^{-8}	0.4252×10^{-6}
25		0.7168×10^{-9}	0.4275×10^{-6}
26		0.4017×10^{-9}	0.3336×10^{-6}
27		0.2103×10^{-9}	0.2120×10^{-6}
28		0.1039×10^{-9}	0.1169×10^{-6}
29			0.6257×10^{-7}
30			0.3936×10^{-7}
31			0.3262×10^{-7}
32			0.3143×10^{-7}
33			0.3029×10^{-7}
34			0.2747×10^{-7}
Total rate	0.9646×10^{-9}	0.1668×10^{-5}	0.1609×10^{-4}

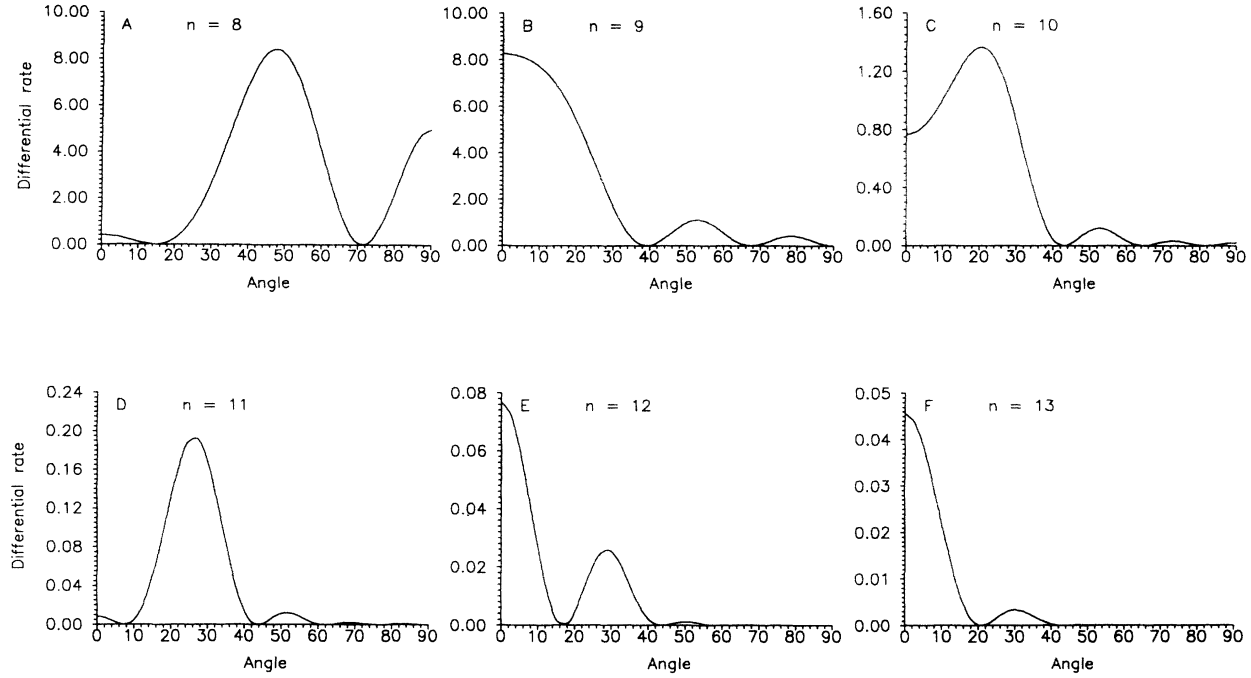

FIG. 5. Electron angular distributions $(1/\sin\vartheta)d\Gamma_n/d\vartheta$ (in units of 10^{-10} a.u.) for the first six above-threshold peaks in the energy spectrum, for the laser intensity 10^{10} W/cm^2 and the wavelength 10.6 μm. Graphs $A-F$ correspond to the number of absorbed photons $n=8-13$, as indicated. The angles are given in degrees.

the total complex-rotated resonance wave functions to the real axis and an exact differential formula. The resonance wave functions can be solved numerically exactly by means of the non-Hermitian Floquet theory and the generalized complex-scaling pseudospectral discretization technique. For laser frequency much smaller than the binding energy, a new nonperturbative adiabatic theory can be employed for efficient and accurate treatment of the resonance wave functions. For the 10.6-μm wavelength of the CO_2 laser used by recent experiments [3], the adiabatic theory is accurate and we extend it to the complex-r domain for the solution of the complex-rotated

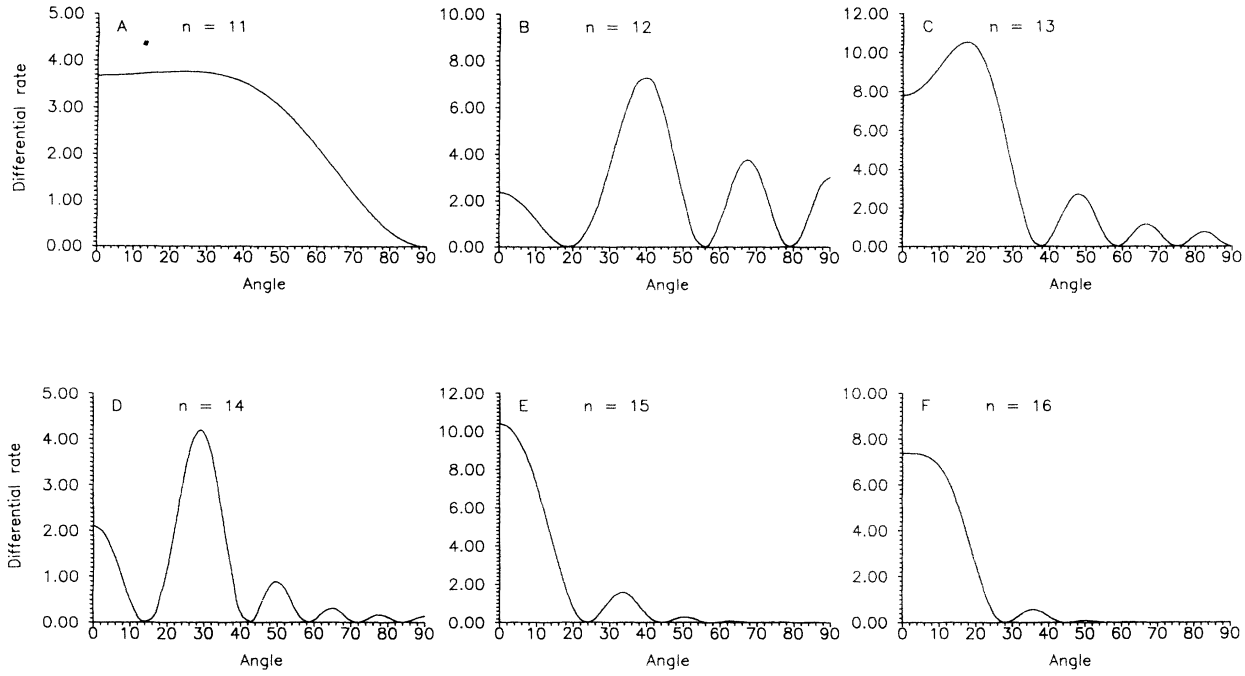

FIG. 6. The same as Fig. 5, for the intensity 5×10^{10} W/cm^2. The differential rates are in units of 10^{-7} a.u.

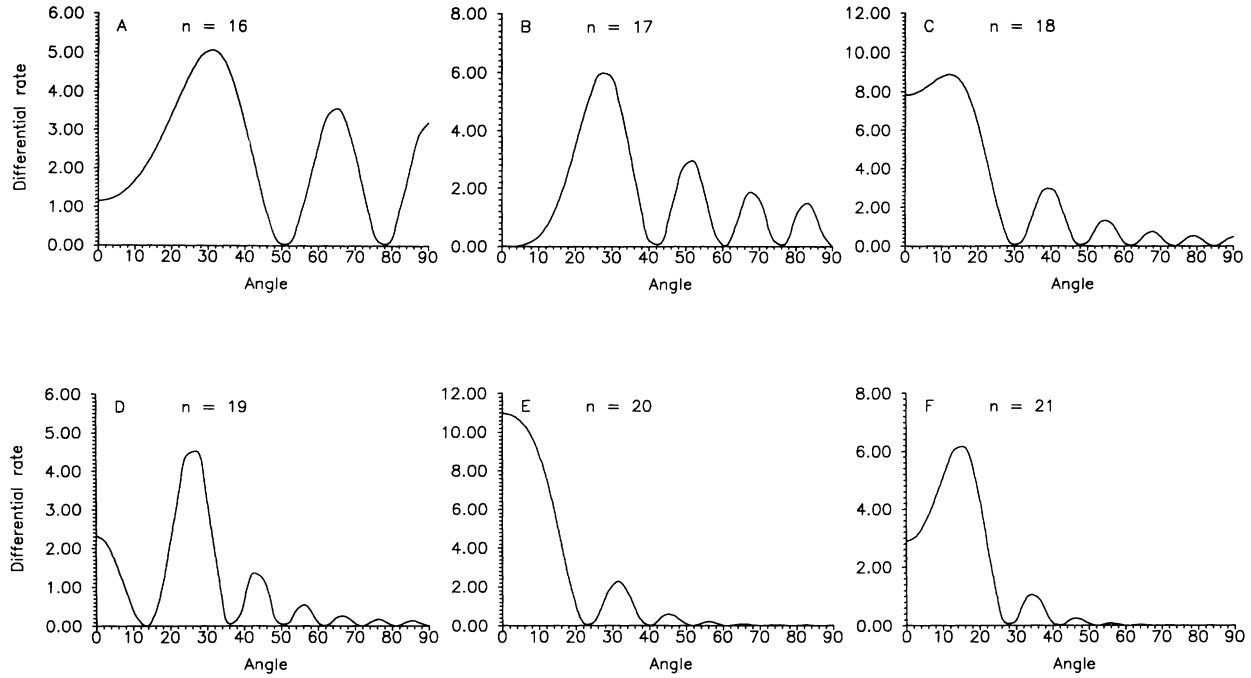

FIG. 7. The same as Fig. 5, for the intensity 10^{11} W/cm^2. The differential rates are in units of 10^{-6} a.u.

quasienergy eigenfunctions for H^- negative ions driven by intense monochromatic laser fields. We perform a detailed study on the angular distribution and partial rates for multiphoton above-threshold detachment of H^- in moderate laser intensities (10^{10}–10^{11} W/cm^2).

Unlike the partial rates, the angular distributions are quite sensitive to the spatial intensity variations inside the laser focus. That is why the pure angular distributions without the spatial disturbances can be observed for rather short laser pulses. In this case the processes that turn on and turn off the laser field should be taken into account. However, we can expect that for such a system as H^- these effects are minimized since they are the most important for quasiresonance processes, and H^- possesses only one bound state. Work is in progress for the detailed study of the effect of laser pulses.

ACKNOWLEDGMENTS

This work was partially supported by the Division of Chemical Sciences, Office of Basic Energy Sciences of the U.S. Department of Energy. One of us (D.A.T.) acknowledges the financial support from the International Science Foundation (Individual Grants Program for the former Soviet Union) and from the Soros Foundation (grant awarded by the American Physical Society).

[1] C. Y. Tang, P. G. Harris, A. H. Mohagheghi, H. C. Bryant, C. R. Quick, J. B. Donahue, R. A. Reeder, S. Cohen, W. W. Smith, and J. E. Stewart, Phys. Rev. A **39**, 6068 (1989).

[2] W. W. Smith, C. Y. Tang, C. R. Quick, H. C. Bryant, P. G. Harris, A. H. Mohagheghi, J. B. Donahue, R. A. Reeder, H. Sharifian, J. E. Stewart, H. Toutounchi, S. Cohen, T. C. Altman, and D. C. Rislove, J. Opt. Soc. Am. B **8**, 17 (1991).

[3] C. Y. Tang, H. C. Bryant, P. G. Harris, A. H. Mohagheghi, R. A. Reeder, H. Sharifian, H. Toutounchi, C. R. Quick, J. B. Donahue, R. A. Reeder, S. Cohen, and W. W. Smith, Phys. Rev. Lett. **66**, 3124 (1991).

[4] For a summary of recent work and a more complete list of references in this direction, see S. Geltman, Phys. Rev. A **43**, 4930 (1991); see also C. R. Liu, B. Gao, and A. F. Starace, *ibid.* **46**, 5985 (1992).

[5] C. Laughlin and S. I. Chu, Phys. Rev. A **48**, 4654 (1993).

[6] J. Wang, S. I. Chu, and C. Laughlin, Phys. Rev. A **50**, 3208 (1994).

[7] K. R. Lykke, K. K. Murray, and W. C. Lineberger, Phys. Rev. A **43**, 6104 (1991).

[8] C. Schwartz, Phys. Rev. **124**, 1468 (1961); A. L. Stewart, J. Phys. B **11**, 3851 (1978); M. R. H. Rudge, *ibid.* **8**, 940 (1975); J. Callaway, Phys. Lett. A **65**, 199 (1978).

[9] A. W. Wishart, J. Phys. B **12**, 3511 (1979); A. L. Stewart, *ibid.* **11**, 3851 (1978).

[10] G. Yao and S. I. Chu, Chem. Phys. Lett. **204**, 381 (1993).

[11] S. I. Chu and W. P. Reinhardt, Phys. Rev. Lett. **39**, 1195 (1977); A. Maquet, S. I. Chu, and W. P. Reinhardt, Phys. Rev. A **27**, 2946 (1983).

[12] For reviews on non-Hermitian Floquet Hamiltonian methods, see S. I. Chu, Adv. At. Mol. Phys. **21**, 197 (1985); Adv. Chem. Phys. **73**, 739 (1989).

[13] H. C. Bryant (private communication).

[14] D. A. Telnov, J. Phys. B **24**, 2967 (1991).

[15] V. N. Ostrovsky and D. A. Telnov, J. Phys. B **20**, 2397 (1987).
[16] L. V. Keldysh, Zh. Eksp. Teor. Fiz. **47**, 1945 (1964) [Sov. Phys. JETP **20**, 1307 (1965)]; F. H. M. Faisal, J. Phys. B **6**, L89 (1973); H. R. Reiss, Phys. Rev. A **22**, 1786 (1980).
[17] A. Dalgarno and J. T. Lewis, Proc. R. Soc. London, Ser. A **233**, 70 (1955).
[18] C. Laughlin (private communication).
[19] N. Moiseyev, F. Bensch, and H. J. Korsch, Phys. Rev. A **42**, 4045 (1990).